

Keywords

Tetrazines,
Anti-inflammatory,
Antibacterial,
Molecular Docking

Received: April 21, 2016

Accepted: May 3, 2016

Published: July 19, 2016

Synthesis, Biological Evaluation and Docking Study of New 1,2,4-Triazolo[4,3-b][1,2,4]Triazines and 1,2,4-Triazolo[4,3b][1,2,4,5]Tetrazines

Labeeb M. Shaif^{1,*}, Faisal M. Aqlan², Khalid O. AL-Footy²,
Waddhaah M. A. Alasbahi¹

¹Department of Chemistry, Faculty of Science, Ibb University, Ibb, Yemen

²Department of Chemistry, Faculty of Science, King Abdul-Aziz Univeristy, Jeddah Kingdom of Saudi Arabia

Email address

labeeb48@hotmail.com (L. M. Shaif)

*Corresponding author

Citation

Labeeb M. Shaif, Faisal M. Aqlan, Khalid O. AL-Footy, Waddhaah M. A. Alasbahi. Synthesis, Biological Evaluation and Docking Study of New 1,2,4-Triazolo[4,3-b][1,2,4]Triazines and 1,2,4-Triazolo[4,3b][1,2,4,5] Tetrazines. *American Journal of Chemistry and Application*. Vol. 3, No. 4, 2016, pp. 19-27.

Abstract

Anovel series of 1,2,4-triazolo[4,3-b][1,2,4]triazines 3-6 and 1,2,4-triazolo[1,2,4,5]tetrazines 8-12 were synthesized by using heterocyclization of 3-(pyridin-4yl)-4-amino-5-substituted amino-1,2,4-triazole (2) and/or 3-(pyridin-4yl)-4-amino-5-hydrazino-1,2,4-triazole (7) with α,β -bifunctional compounds such as chloromethyl diphenyl phosphonic acid phenacyl bromide, pyruvic acid, diethyl oxalate, triethyl phosphite, triethyl orthoformate, fluorinated benzaldehydes, ethylchloroformate and carbon disulfide in different conditions. Moreover, compounds 3, 6, 8, 7, 9, 10, 11 and 12 displayed high inhibition against all bacteria tested in compared with the standard antibiotic Indomethacin. The newly synthesized compounds were evaluated for their *in vivo* anti-inflammatory activities and the results revealed that the compounds 7, 8, 10 and 12 have high % inhibition of edema as compared to standard drug (Indomethacin). Molecular docking studies were performed in order to investigate the plausible binding modes of synthesized compounds 8 and 10 into the active sites of enzyme COX-II.

1. Introduction

Triazines derivatives as nonsteroidal drugs demonstrate a broad range of biological activities such as Tirapazamine as anti-tumor [1], Lamotrigine as anti-epileptic drug [2], and fused 1,2,4-triazines as anti-microbial [3-5], anti-HIV [6], anti-mycobacterial [7], anti-viral [8], anxiolytic [9] and anti-depressant [10] agents are already reported in literature. Heterobicyclic nitrogen systems containing 1,2,4-triazine moiety have also shown anti-HIV and anticancer activities [11,12]. Similarly, 1,2,4-triazole systems containing 1,2,4-triazine moiety are an important class of heterocyclic analogues with various pharmacological activities such as anti-inflammatory and antimicrobial activities.

In the light of these observations this prompted researchers to design synthesis of the new drugs contain heterocyclic compounds (spatially tetrazine and triazole rings) due to

the difficulty in the construction of N–N bond by living organisms and it's the rapeutic activities.

Recently, Abdel–Rahmanetal [13,14] reported that 1,2,4-triazole, 1,2,4-triazines and/or 1,2,4-triazolo–1,2,4,5-tetrazines as antimicrobial and anticancer drugs as well as has molluscicidal activity.

Inhibition of cyclooxygenase (COX) produces different types of the rapeutic biological effects, as there are different isoenzymes COX–I and COX–II. Both types of cyclooxygenases have a hydrophobic tunnel or cavity, through which the substrate accesses the activesite. The tunnel is larger in the COX–II isoenzyme with a side pocket, aproperty exploited in the development of specific COX–II inhibitors [15]. Compelling evidence suggests that inhibition of prostanoids produced by COX–II can be ascribed to the anti-inflammatory, analgesic and antipyretic effects of NSAIDs. Because of that it is considered a potential target for the treatment of inflammation [16] and the design of selective COX–II inhibitors should provide relief from the symptoms of inflammation and pain.

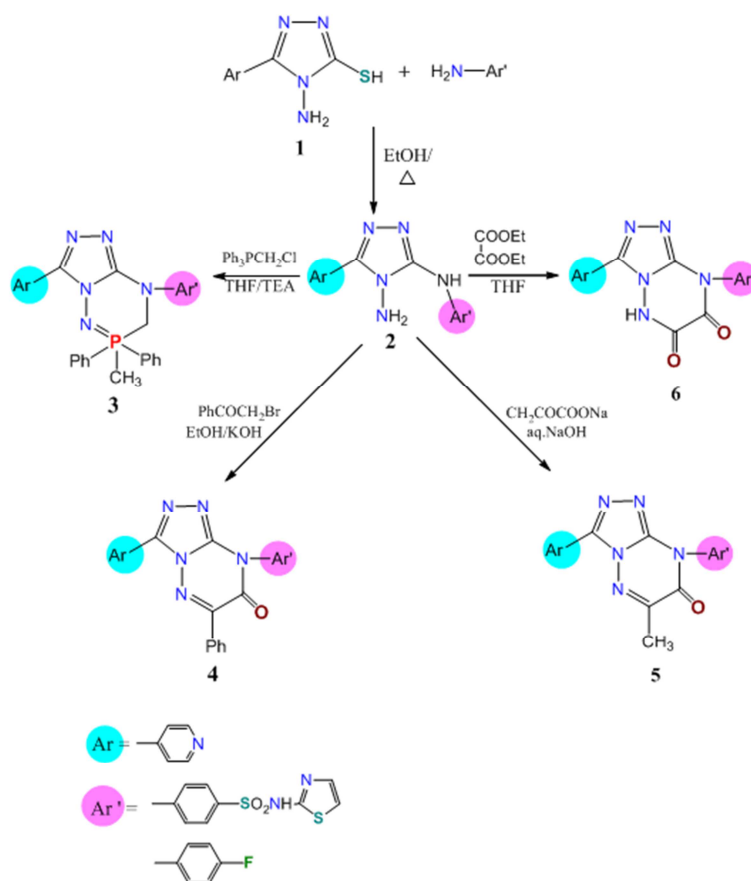
In this study, synthesis of some newer fused heterocyclic systems derived from 5-substituted amino–4-amino–3-

(pyrid–4-yl)–4H–1,2,4-triazole (2) with view of their anti-inflammatory and antimicrobial activities. Molecular modeling studies were carried out in order to prove whether COX–II was a possible target for the our newly synthesized compounds.

2. Results and Discussion

2.1. Chemistry

A simple nucleophilic displacement of mercapto group by primary aromatic amines as p-fluoroaniline and/or sulfathiazole against 4-amino–5-mercapto–3-(pyrid–4-yl)–1,2,4-triazole (1) in boiling isopropanole yielded 4-amino–5-substitutedamino–1,2,4-triazole derivatives (2a,b). structures of 2 were deduced mainly from is appeared of mercapto functional group at 2600–2500 cm^{-1} in the IR. $^1\text{HNMR}$ spectra showed the new NH proton of aromatic amines at $\delta 14.22$ ppm with NH_2 proton of aminotriazole at 5.87 ppm. Also, UV absorption of 2 a exhibit λ_{max} at 374 nm while that of 1 at 317 nm, which confirm that new structure of 2 (Scheme1).



Scheme 1. Synthetic pathway of compounds 1–6.

Ring closure reactions of compound 2 with diphenyl (chloromethyl)phosphrous oxide in stirring with THF followed by warming afforded [17] 3,8-diaryl–4,5,6,7-tetrahydro–6-hydroxy–1,2,4-triazolo[4,3b][1,2,3,5] phosph

triazine (3) (Scheme1). Structure of 3 was deduced from presence of p–OH, P–N and NH functional groups at 1653,1105,1039,945 and 3200 cm^{-1} in that IR spectrum. $^1\text{HNMR}$ spectrum gives supported that structure which

exhibited a resonated signals at δ 3.15 (b,1H,CH₂-p), 3.98–3.99 (m,2N,CNP) and 11ppm (b,1H,NHP).

1,2,4-Triazolo[4,3-b][1,2,4]-triazine derivatives 4–6 have been obtained from heterocyclizaion of compound 2 with phenacylbromide (KOH), sodiumpyruvate (NaOH) and diethyloxalate (THF/DMF) under reflux (Scheme1).

Structures of compounds 4–6 were deduced from both the elemental analysis and spectral measurements. IR spectrum of 4 showed a characteristic bands at γ 2980,1429 (str.andbendingCH₂). While, that of 5 recorded γ at 2978,1480 (str. And bending of CH₃), 1768 (C=O), in addition that of 6 recorded γ at 3250 (NH), 1769, 1631 (2C=O) with a bands of C–F, C=N and substituted pyridine and aromatic rings, 1212,850–730 cm⁻¹.

One of the importance aims of the presentis discovery a higher potency new 1,2,4-triazolo[1,2,4,5]tetrazine system sa santi-inflammatory and antimicrobial agents. Refluxing compound 1 with hydrazine hydrate in ethanol yielded the 4-amino-5-hydrazino-3-(pyrid-4-yl)-1,2,4-triazine (7) as starting material for the building of some new 1,2,4-triazolo-tetrazines. A hydrazine group is more nucleophilic and basic character than amino group in the compound 7. Thus, orientation of cyclization firstly from hydrazine center followed by amino center (Scheme 2).

3-Aryl-7,8-dihydro-1,2,4-triazolo[4,3-c][1,2,3,5,6]phosphate-tetrazine 8 was obtained from refluxing

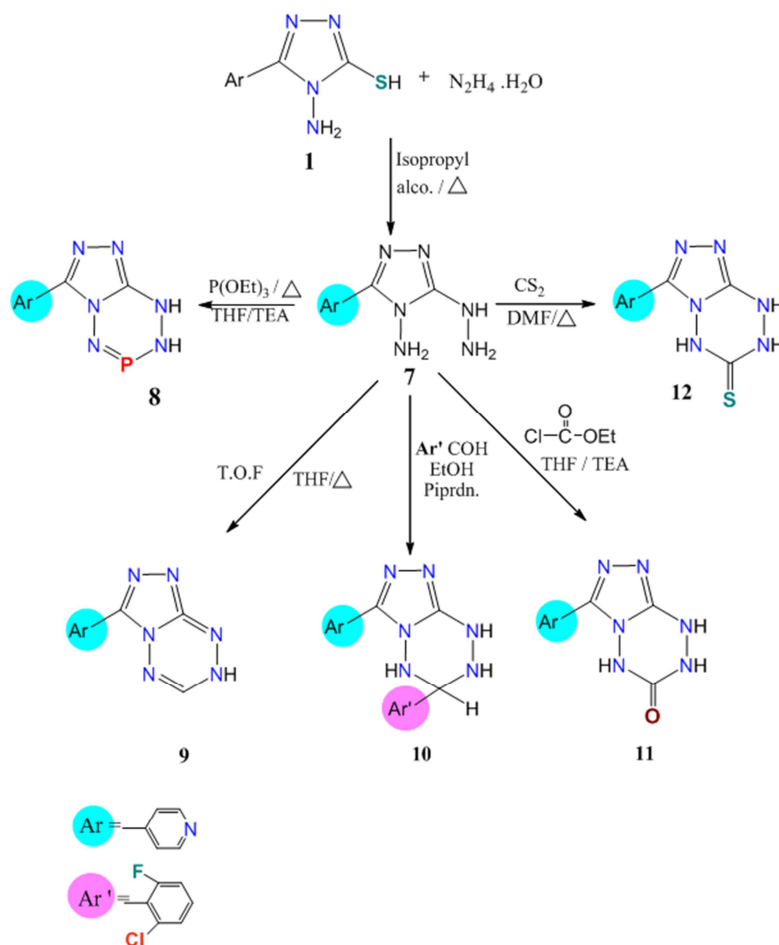
compound 7 with triethyl phosphine in THF, while treatment of 7 with triethylorthoformate under these conditions, produced

3-aryl-7,8-dihydro-1,2,4-triazolo[4,3-b][1,2,4,5]tetrazine 9. Also cycloaddition reaction of 7 with aromatic aldehyde in boiling ethanol with a few drops of piperidine, furnished 3,6-diaryl-5,6,7,8-tetrahydro-1,2,4-triazolo[4,3-b][1,2,4,5]tetrazine 10 (Scheme 2).

Former structure of 8–10 was elucidated from its IR absorption spectrum, were reported a characteristic bands γ 3100–2950 cm⁻¹ (1) (NH, NH) of 8 and 9 at γ 3269, 3158 and 3100 cm⁻¹ (1) (3HN) of 10, in additional a bands at γ 1602, 1568 cm⁻¹ (p=N, C=N).1216 (C–F) and 321, 734 cm⁻¹ of substituted pyridine aromatic moieties. MS of 8 recorded M⁺ at 219 (221, M+1) and 193 (100).

UV absorption spectra of both the compounds 2 and 10 give us another induction for the inhibition of electronic transition after heterocyclization. Thus, λ_{max} of 2 was 311 nm while that of 10 was 267 and 261 nm.

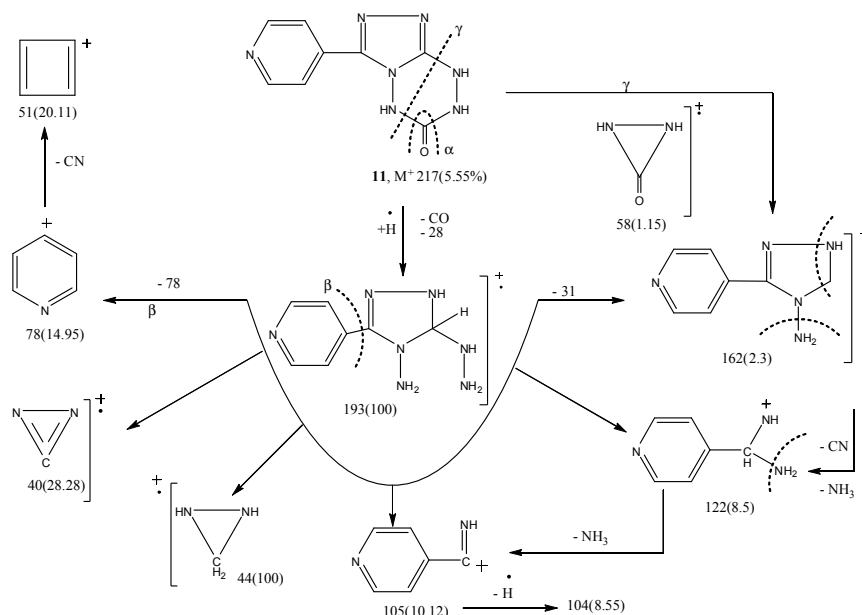
Finally,1,2,4-triazolo[4,3-b][1,2,4,5]tetrazine5(4H)one/thione 11 and 12 were synthesized from refluxing 5-hydrazine-4-amino-1,2,4-triazole (7) with triethylortho formote (TEA/THF) and /or with CS₂ (in DMF) (Scheme 2). Formation of compound 11 may be deduced *via* esterification of 7 followed by elimination of one mole of ethanol, while formation of 12 via addition to S=C=S followed by elimination of H₂S [18].



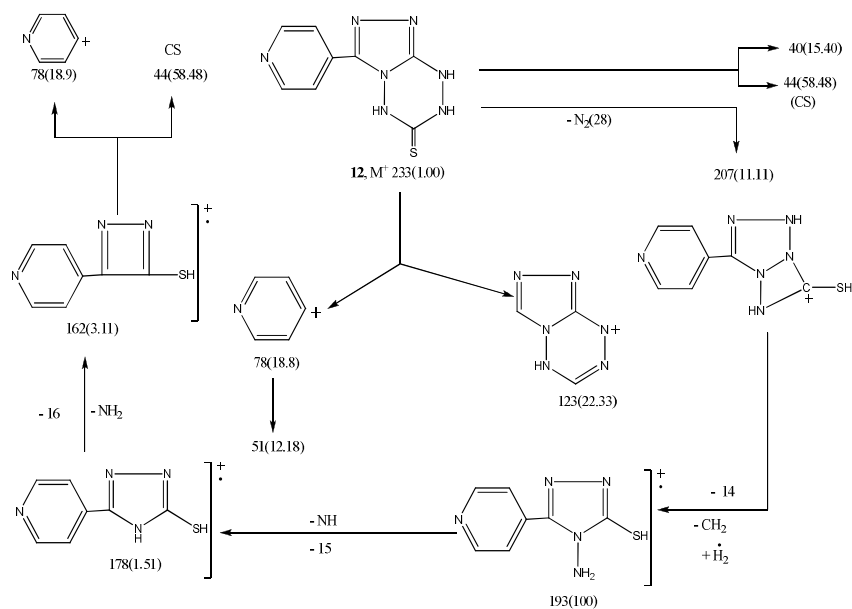
Scheme 2. Synthetic pathway of the targeted compounds 7–12.

Structures of 11 and 12 were deduced from their elemental and spectral analysis. That IR absorption spectra of γ recorded γ at 3149(b,NH,NH), 1624(CONH), while that 12 showed a bands at 3269,3158(NH,NH), 2402 (b,SH \leftrightarrow NH), In addition at 1602,1308,820,733 cm^{-1} which attributed to C=N,NCSN and substituted pyridine. ^1H NMR spectrum of 12 recorded a signals at δ 2.5(τ , ^1H ,NH 1 of tetrazine), 14.21 ppm(τ , ^1H ,NH 2 of tetrazine), with δ 5.8 of SH proton. ^{13}C Nmr

give us a good indication of structure which showed a resonated signals at δ 169(C $_1$ of C=S), 148(C $_2$,C $_3$ of triazole), 134(C $_4$ of pyridyl) and 122,121,151,150 ppm of pyridine carbons. MS of both the compounds 11 and 12 exhibited M $^+$ at 217(5.55) for 11 and at 233(1.00) for 12, with a base peak at 193 for both compounds 11 and 12 which confirm their structure [Schemes 3&4].



Scheme 3. Mass Fragmentation pattern of compound 11.



Scheme 4. Mass Fragmentation pattern of compound 12.

2.2. Biological Evaluation

Recently, much attention has been focused on bridgehead nitrogen heterocycles especially containing 1,2,4-triazole, 1,2,4-triazine and 1,2,4,5-tetrazine derivatives due to their wide applications especially in medicine area. In view of the

observations, the aim of this work is synthetic some new fused 1,2,4-triazole with 1,2,4-triazine / 1,2,4,5-tetrazine nucleus containing a various functional groups in an attempt to enhance that antimicrobial and anti-inflammatory activities.

2.2.1. Antimicrobial Activity

The newly synthesized compound have been evaluated for antibacterial activity against *Escherichia coli* and *Pseudomonas aeruginosa* as (-ve) bacteria *Staphylococcus aureus* as (+ve) bacteria, in addition, *Candida albicans* fungi using applied standard method [19]. DMF was used solvent for Nystatin which act as reference drug for bacteria and fungi. The MIC (Minimum inhibitory concentration) was defined as the lowest concentration of the tested compounds at which no growth of the strain was observed in a period of time and under specified experimental conditions. The inhibition MIC values for the screening was reported in Table 1 and figure 1. It was noticed that the synthesized compounds significantly inhibited the high activity against fungi used *C. albicans* in compare with Nystatin. All the tested compounds recorded high to moderate activities against bacteria used *E. coli*, *P. aeruginosa* and *S. aureus* in compare with Nystatin 50 µg/discs. Compounds 3,6, and 12 showed higher activities against bacteria *E. coli* at concentration 50 µg/disc, the higher activity of the compounds 3,6 and 12 is mainly due to these compounds containing a fluorine, chlorine and phosphorus elements within the structure of 1,2,4-triazine and 1,2,4,5-tetrazine, chlorine and phosphorus elements within the structure of 1,2,4-triazine and 1,2,4,5-tetrazine.

Table 1. The Antimicrobial Activity Screening of Some New Synthesized Compounds.

MIC	Inhibition Zone (mm)*			fungi
	<i>E. coli</i>	<i>P. aeruginosa</i>	<i>S. aureus</i>	
Compound No.				<i>C. albicans</i>
3	19	20	–	14
6	13	–	–	13
8	11	–	–	13
9	11	–	–	12
7	11	11	–	12
10	11	11	–	12
11	16	11	–	12
12	13	11	–	11
Nystatin	–	15	17	–

*Concentration: 100,50 and 25 µg/disc.

Highly active: IZ ≥ 12

Moderately active: IZ = 9–12

Slightly active: IZ = 6–9; Not sensitive; IZ < 6 mm

MIC: minimum Inhibitory Concentration at 50 and 25 µg/disc.

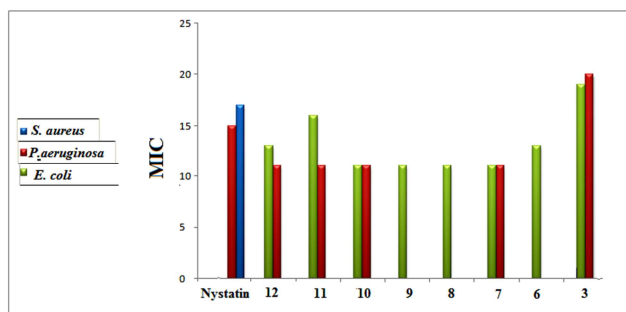


Fig. 1. MIC comparison of the antibacterial activity of some tested compounds with Nystatin.

2.2.2. Anti-inflammatory Activity

Carrageenan-induced paw edema model was used for studying anti-inflammatory activity [20]. As shown in Table 2 and figure 2, the selected of some tested compounds (7, 8, 10 and 12) were evaluated via carrageenan-induced paw edema protocol at hourly intervals for 3 hours (0, 1, 2, 3 h) compared to the reference drug (indomethacin) were determined as the increase in paw edema volume [13, 14].

The percent of inhibition of inflammation was determined using formula:

$$= \frac{\text{wt. of paw edema of control} - \text{wt. of paw edema of related}}{\text{wt. of paw edema of control}} \times 100$$

In table 2, Compounds 8 and 10 revealed higher anti-inflammatory activity that exceed the activity of indomethacin itself with 32.22% and 36.55% inhibition, respectively, On the other hand, compound 7 showed a slightly lower anti-inflammatory activity than indomethacin. Compound 12 did not produce significant anti-inflammatory activity. The reason of this results, compounds 8 and 10 carrying phenyl groups containing both the fluorine and chlorine elements are active against anti-inflammation, in compare the standard antibiotic used (Indomethacin). Both the compounds 8 and 10 containing mainly s-triazolo and s-tetrazine with presence of both phosphorus and fluorine elements, in incorporated with pyridyl moiety. A higher activity of the titled prepared compounds is agreement to the recent results in the area of phosphorus – fluorine bearing a heterocyclic nitrogen systems.

Table 2. The anti-inflammatory activity of the tested compounds (20mg/kg.b.w) and Indomethacin (5mg/kg.b.w).

Treatment	Mean increase in paw volume (ml)				% Inhibition in paw
	0h	1h	2h	3h	
Control	0.66±0.05	0.69±0.04	0.76±0.06	0.81±0.05	–
Indomethacin	0.22±0.02	0.24±0.01	0.27±0.02	0.29±0.03	45.19*
7	0.36±0.03	0.38±0.02	0.39±0.02	0.41±0.03	30.38 ^s
8	0.32±0.05	0.34±0.06	0.35±0.06	0.36±0.04	36.55*
10	0.55±0.05	0.58±0.06	0.61±0.05	0.63±0.06	32.22*
12	0.58±0.05	0.61±0.06	0.63±0.05	0.64±0.05	19.87 [#]

± S.E.: Mean Standard Control.

#p>0.05 (no significant difference), Sp<0.05 (moderate significant difference), *p<0.001 (significant difference)

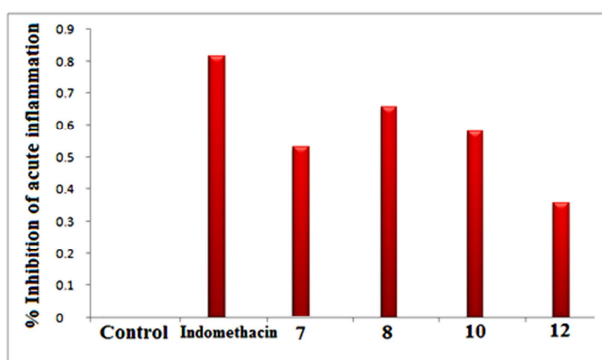


Fig. 2. % Inhibition of acute inflammation (carrageenan-induced pawedema).

2.3. Molecular Modeling Studies (Structure Based Drug Design)

Molecular docking technique was employed to evaluate the anti-inflammatory behavior of compounds with COX-II selective inhibition enzyme [21].

The active site of COX-II is divided into three important regions: the first region being a hydrophobic pocket defined by Tyr385, Trp387, Phe518, Ala201, Tyr248 and Leu352, the second region being the entrance of the active site lined with the hydrophilic residues Arg120, Glu524, Tyr355 and the third is a side pocket lined by His90, Arg513 and Val523 (Fig. 3) [22]. The scoring functions and hydrogen bonds formed with the surrounding amino acids are used to predict their binding modes, their binding affinities and orientation of these compounds at the active site of the COX-II enzyme (pdb code: 3NT1) were characterized. Compounds 8 and 10 were having stronger binding interactions with the residues of COX-II protein than the rest of the series.

Increased docking scores are due to enhanced occupancy of triazine and tetrazine moieties of our compounds in the side pocket of the binding site of COX-II created by Gly532, Ser121, Leu117 and Ser126; which are further supported by high lipophilic, Van der Waals interactions and hydrophobic enclosure with the residues of the COX-II protein. The compound 8 forms H-bonding interactions at the triazine ring: NH of Ser120 and with NH of Lys532, also the compound 10 forms H-bonding interactions at the tetrazine ring with NH of Tyr136 and Ala156. With all these evidences it shows that our compounds are selective for COX-II protein which is in agreement with anti-inflammatory activity.

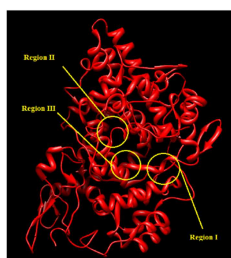
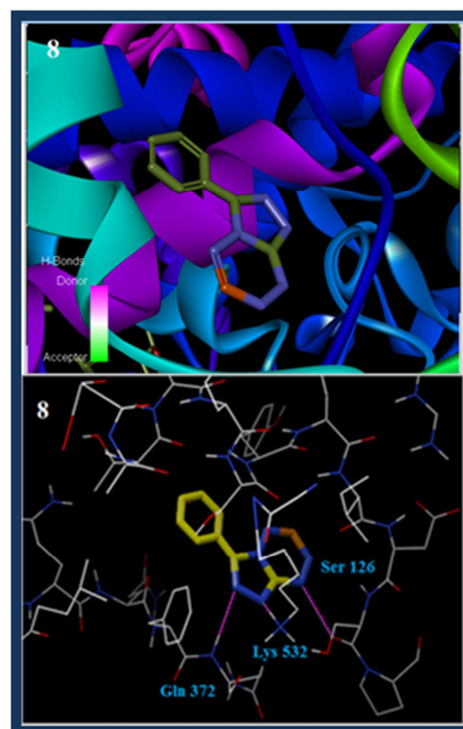
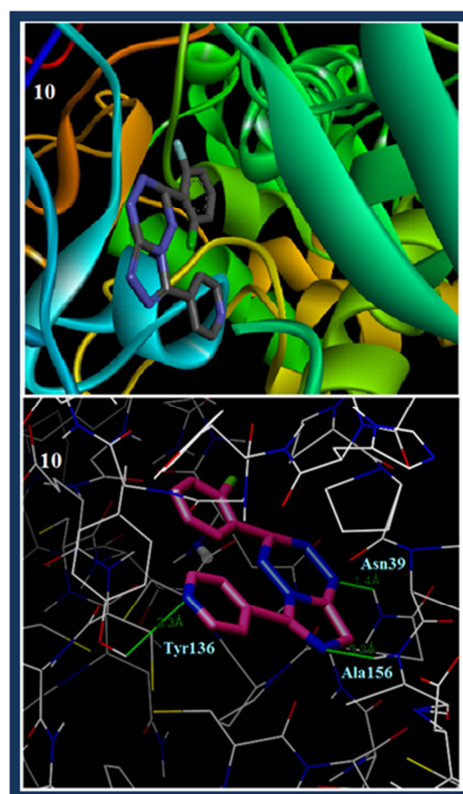


Fig. 3. Modeling of X-ray crystallographic structure of COX-II (PDBID:3NT1). The classical binding site were marked in the corresponding location.



(a)



(b)

Fig. 4. Molecular docked model of compounds 8 (a) and 10 (b) (stick presentation) located within the active sites of COX-II enzyme; compounds represented in a wire form and the green line showing hydrogen bond interaction between compounds 8 and 10 and COX-II enzyme.

3. Material and Methods

3.1. Chemistry

The IR spectra recorded for KBr discs on a Perkin Elmer Spectrum RXI FT-IR systems No. 55529. $^1\text{H}/^{13}\text{C}$ -NMR were determined for solution in deuterated DMSO with a Bruker NMR Advance DPX 400 MH using TMS as an internal standard solvent. Mass spectra were measured on a GCMS-Q 1000 Ex spectrometer. Electronic absorption spectra were recorded in DMF on Shimadzu UV and visible 3101 PC spectrophotometer. Melting points were determined in an electrothermal Bibby Stuart Scientific melting point SMP (US). Microanalyses (CHNS elemental analyzer) and the anti-inflammatory and antimicrobial evaluation were carried out in Department of pharmaceutical Microbiology, National Center for Radiation Research and Technology, Nasr City, Egypt. Thin layer chromatography (TLC) was performed (on silica gel GF254, Merck, Germany) to monitor progress of the reaction and purity of the compounds. Spot being located using either iodine vapors. Compound 1 was prepared according to the reported method¹¹ by direct hydrazinolysis of 4-pyridyl-CONHNHCS₂K.

3.1.1. Synthesis of 5-arylamino-4-amino-3-(pyrid-4-yl)-1,2,4-triazoles (2a,b)

An Equimolar mixture of 1 and 4-fluoroaniline and/or sulfathiazole in DMF-ethanol (1:1, 100ml) was refluxed for 4h, cooled then poured into ice. The produced solid was filtered crystallized to give 2a and/or 2b respectively.

2a: Yield 74% (crystal from dioxan); m.p.2 20-222°C, Anal. Calcd. for C₁₃H₁₁N₆F: C,57.77;H,4.07;N,31.11. Found: C, 56.90; H, 3.98; N, 30.17.

2b: yield 75% (crystal from DMF); m.p. 210-212°C, Anal. Calcd. for C₁₆H₁₄N₈S₂O₂: C, 46.37; H, 3.38; N, 27.05; S, 15.45. Found: C, 45.44; H, 3.31; N, 26.45; S, 15.06. Uv-vis absorption: $\lambda_{\text{max}}/\text{nm}$ ($\epsilon/10^3 \text{ M}^{-1} \text{ cm}^{-1}$): 374 (0.85) nm. Selected IR data on KBr (ν_{max} , cm^{-1}): 3250, 3130 (NH₂, NH), 16010, 1585 (C=N), 1250 (C-F), 830, 780 (aromatic CH, pyridine CH) and 705 cm^{-1} (C-F), ¹HNMR (DMSO-d₆, 400 MH), δ ppm: 5.87 (τ , 2H, NH₂); 7.2, 7.4 (each τ , 4H, aromatic protons); 7.82, 8.041 (each τ , 2H of pyridine); 8.77, 8.81 (each τ , 2H of pyridine); and at 14.22 ppm (NH of substituted amino). ¹³CNMR (DMSO-d₆) δ ppm: 158 (C₁ of C-F); 115.13, 114.99 (C₂ & C₃ of aryl); 119.58, 119.99 (C₄ & C₅ of aryl); 132.99 (C₆ of aryl), 147.36 (C₃ & C₅ of triazole); 129.75 (C₅ of pyridine); 121.63 (C₃ & C₅ of pyridine); 150.82, 150.04 ppm (C₂ & C₆ of pyridine). ESI-MS (m/z, Int.%): 270 (5.5), 253 (5.21), 226 (4.21), 207 (37.71), 165 (5.8), 103 (4.85), 78 (2.11), 44 (100), 40 (12.18).

3.1.2. Synthetic of 3,8-diaryl-4,5,6,7-tetrahydro-6-diphenyl-6-hydroxy-1,2,4-triazolo[4,3-b][1,2,3,5]Phosphatriazine(3)

A mixture of 2a (0.01mol) and diphenyl chlorophosphin oxide (0.01mol) in THF (100ml) with TEA (0.5ml) was refluxed for 4h, cooled. The obtained solid filtered and

crystallized to give 3. Yield 86%, (crystals from dioxin); m.p.300-303°C. Anal.Calcd. for C₂₆H₂₂N₆PO: C,64.46; H,4.54; N,17.35. Found: C, 64.37; H, 4.47; N,17.17. Selected IR data on KBr (ν_{max} , cm^{-1}): 3084(aromatic CH), 2922.68(aliphatic CH), 1653(P-OH), 1510(C=N), 1433(deformation of CH₂), 1388,1344(N-N-C-N), 1105.66,1039,945(P-N), 851, and 8.04(aryl CH) 667.84. ¹HNMR (DMSO-d₆, 400 MH): δ ppm: 3.15(b,1H,CH₂-P), 3.98-3.99(2H,m,CH-P), 7.1-7.45(m,14H, aromatic protons), 7.8,8.2(each d,4H of pyridine), 11.0(b,1H,NHP), and 14.4 ppm (τ ,1H,OH-P).

3.1.3. Synthetic 6,7-dihydro-3-(pyrid-4-yl)-8-aryl-1,2,4-triazolo[4,3-b][1,2,4]triazine(4)

A mixture of 2 (0.01mol) and phenacyl bromide (0.01mol) in ethanolic KOH (5%, 50ml) was warmed under reflux for 2h, and cooled. The reaction mixture was poured into ice-HCl. The yielded solid was filtered and crystallization to give 4. Yield 88% (crystals from dioxin with dill. MeOH), m.p.185-187°C. Anal.Calcd. for C₂₁H₁₅N₆F: C,68.18; H,4.05; N, 22.70. Found: C,67.81; H,4.00; N,22.24. Selected IR data on KBr(ν_{max} , cm^{-1}): 3099.20 and 2980 (aromatic and aliphatic of CH), 1527(C=N), 1429(deformation of CH₂), 1283(C-F), 930,832(aryl CH) and 688 (C-F).

3.1.4. Synthesis of 3,8-diaryl-6-methyl-1,2,4-triazolo[4,3-b][1,2,4]-triazin-7-one (5)

A mixture of 2a (0.01mol) and sodium pyruvate (0.01mol, in H₂O 10ml)with aqueous NaOH (5%, 50ml) was refluxed for 2h, cooled then poured into ice-HCl. The produced was filtered and crystallized to give 5. Yield 75% (crystal from EtOH), m.p.300-302°C. Anal.Calcd. for C₁₆H₁₁N₆FO: C, 59.62; H,3.41; N,26.08. Found: C,58.99; H,3.34; N,25.95. Selected IR data on KBr(ν_{max} , cm^{-1}): 3090, 2978 cm^{-1} (aromatic and aliphatic CH), 1768 (C=O), 1592 (C=N), 1480.95 (deformation of CH₃), 1322(N-N-C-N), 1213(C-F), 836, 816, 762,729 (aromatic & pyridine CH), and 675 (C-F). ESI-MS (m/z, Int.%): 322(M⁺,2.50), 294(44.5), 268(12.2),179(100), 154(1.10), 147(13.01), 104(20.1), 108(1.1), 78(58.9), 44 (27.74), 40(6.73).

3.1.5. Synthesis of 3,8-diaryl-1,2,4-triazolo[4,3-b][1,2,4]triazin-6,7-(5H)dione (6)

Equimolar mixture of 2a and diethyl oxalate in THF (100ml) was refluxed for 4h, cooled. The obtained solid was filtered and crystallized to give 6. Yield 79% (crystal from EtOH), m.p.183-185°C. Anal.Calcd. for C₁₅H₉N₆FO₂: C, 55.55; H,2.77; N, 25.84. Found: C, 54.99; H,2.71; N,25.49. Selected IR data on KBr(ν_{max} , cm^{-1}): 3250(NH), 3085 (aromatic CH), 2699.50 (C-OH), 1769,1631.49(2C=O), 1592,1547(C=N), 1212 (C-F), 836,818,762,729(aromatic and pyridine CH).

3.1.6. Preparation of 3-(pyrid-4yl)-4-amino-5-hydrazino-1,2,4-triazole (7)

A mixture of 1 (0.01 mol) and hydrazine hydrate (0.04mol)

in ethanol (100ml) was refluxed for 4h, cooled then added a few drops acetic acid. The produced solid was filtered and crystallized to give 7. Yield 81% (crystal from EtOH); m.p.140–142°C. Anal.Calcd. for C₇H₉N₇: C,43.97; H,4.71; N,51.30. Found: C,43.81; H,4.61; N,50.93. Uv–vis absorption: λ_{\max}/nm ($\epsilon/10^3 \text{ M}^{-1} \text{ cm}^{-1}$): 311(2.2). Selected IR data on KBr(ν_{\max} , cm^{-1}): 3350 (NH₂), 3159(NH), 3080(aromatic CH), 1605(deformation NH₂), 1570(C=N), 1313(N–N–CN), and 822,735,707,687(4CH of pyridine). ¹HNMR (DMSO–d₆,400 MH), δ ppm: 4.3(τ ,2H,NH₂ of hydrazino), 5.85(τ ,2H,NH₂ of 1,2,4–triazole), 7.82,7.83(each τ ,2H of pyridine), 8.85,8.81(each τ ,2H of pyridine), and 14.2 ppm (τ ,1H,NH₂ of hydrazino).

3.1.7. Synthesis of 3-Aryl-7,8-dihydro-1,2,4-triazolo[4,3-*c*][1,2,3,5,6]Phosphatetrazine (8)

Equimolar of 7 and triethylphosphite in THF (100ml) and TEA (0.5ml) was refluxed 4h, cooled. The obtained solid was filtered and crystallized to give 8. Yield 74% (crystal from THF); m.p.236–237°C. Anal.Calcd. for C₇H₆N₇: C, 38.35; H,2.73; N,44.74. Found: C, 37.98; H,2.70; N,44.49. Selected IR data on KBr(ν_{\max} , cm^{-1}): 3100–2950 (br,NH–NH), 1651(P–NH), 1588 (C=N), 1358(NCN), 100,1050,950 (P–N), 832,785,710 and 689 (pyridine CH).ESI–MS (m/z, Int.%): 219(221,M⁺,(1.50)), 193(100), 162(41), 147(1.10), 78(18.10), 44(100), 40(30.08).

3.1.8. Synthesis of 3-aryl-7,8-dihydro-1,2,4-triazolo[4,3-*b*][1,2,4,5] tetrazine (9)

A mixture of 7 (0.01mol) and triethylorthoformate (0.012mol) in THF (100ml) was refluxed for 4h, cooled. The produced solid was filtered and crystallized to give 9. Yield 70% (crystal from dioxan); m.p.230–231°C. Anal.Calcd. for C₈H₇N₇: C,47.76; H,3.48; N,48.75. Found: C,47.44; H,3.41; N,48.42. Selected IR data on KBr(ν_{\max} , cm^{-1}): 3150, 3105(NH,NH of tetrazine&triazole), 1610, 1588(C=N), 1348(NCN), 850,820,730,710 and 690 (pyridine CH). 201(0.01%),193(100), 163(15.0),147(2.10), 105(22.8), 122(12.1), 78(28.1), 44(40.15), 40(12.12).

3.1.9. Synthetic 3,6-diaryl-5,6,7,8-tetrahydro-1,2,4-triazolo[4,3-*b*][1,2,4,5] tetrazine (10)

A mixture of 7 (0.01mol) and 2-chloro-6-fluorobenzaldehyde (0.01mol) in ethanol (100ml).piperidine (0.5ml) was refluxed 12h, then cooled. The produced solid was filtered and crystallized to give 10. Yield 72% (crystal from dioxan); m.p.237–239°C. Anal.Calcd. for C₁₄H₁₁N₇Cl: C,5.75; H,3.32; N,29.60. Found: C,50.44; H,3.25; N,29.41. Uv–vis absorption: λ_{\max}/nm ($\epsilon/10^3 \text{ M}^{-1} \text{ cm}^{-1}$): 267(1.11) and 261 (1.01). Selected IR data on KBr(ν_{\max} , cm^{-1}): 3296,3158 and 3100 (3NH), 3020(aromatic CH), 1602,1568 (C=N), 13.9(N–N–C–N), 1216(C–F), 821,734 (aromatic and pyridine CH), 685 (C–Cl). ¹³CNMR (DMSO–d₆), δ ppm: 147(C₃,C₅of triazole), 133,122,211,151 and 150 (five carbons of pyridine), 136,134(C–F& C–Cl of aryl), 45(C₆ of –CH–tetrazine) and 129,128 (four carbons of aryl).

3.1.10. Synthetic 3-aryl-7,8-dihydro-1,2,4-triazolo[4,3-*b*][1,2,4,5]tetrazin-6(4H)one(11) and Synthetic 3-aryl-7,8-dihydro-1,2,4-triazolo[4,3-*b*][1,2,4,5] tetrazin-6 (4H)thione (12)

A mixture of 7 (0.01mol) and ethyl chloroformate (0.012mol) with THF (100ml) and TEA(0.5ml, added dropwise) was refluxed for 2h, then cooled. Then obtained solid was filtered and crystallized to give 11. Yield 71% (crystal from EtOH); m.p.170–171°C. Anal.Calcd. for C₈H₇N₇O: C, 44.23; H,3.22; N,45.16. Found: C, 43.56; H,3.17; N,44.69. Uv–vis absorption: λ_{\max}/nm ($\epsilon/10^3 \text{ M}^{-1} \text{ cm}^{-1}$): 326 (1.31). Selected IR data on KBr(ν_{\max} , cm^{-1}): 3149(b, NH–NH), 1624(–CONH), 1582(C=N), 1358(N–N–C–N), and 787,739 (pyridine CH).ESI–MS (m/z, Int.%):217(5.55), 193(100), 162(2.30), 104(8.55), 78(14.95), 44(100), 40(28.28). Also a mixture of 7 (0.01mol), CS₂ (0.02mol) in DMF (50ml) was refluxed for 2h, cooled. Then poured onto ice. The resulted solid was filtered and crystallized to give 12.Yield 84% (crystal from THF); m.p.238–240°C, Anal. Calcd. for C₈H₇N₇S: C,41.20; H,3.00; N,42.06; S,13.73. Found: C, 40.90; H,2.96; N,41.86; S,13.44. Uv–vis absorption: λ_{\max}/nm ($\epsilon/10^3 \text{ M}^{-1} \text{ cm}^{-1}$): 316(1.5). Selected IR data on KBr(ν_{\max} , cm^{-1}): 3296,3158(NHNH), 2402,1812 (b, $\bar{\nu}$ --- $\overset{|}{\text{N}}\text{H}_2$),1602(C=N), 1308(NCSN), 820 and 733 (pyridine CH).¹HNMR (DMSO–d₆,400 MH), δ ppm: 2.5(τ ,1H, –NH– tetrazine), 5.8(τ ,1H,SH), 8.031 & 8.76(each τ ,4H of pyridine), and 14.21 ppm(τ ,1H,²NH of tetrazine). ¹³CNMR (DMSO–d₆), δ ppm: 169(C₁ of C=S), 148(C₂, C₃ of 1,2,4–triazole), 134(C₄ of pyridin–4–yl), 122.121(C₃, C₅ of pyridine), 151.150 (C₂, C₆ of pyridine).ESI–MS (m/z, Int.%):233(1.00%), 193(100), 178(1.51),162(3.30), 122(4.20), 106(15.15),78(18.9), 44(58.48), 40(15.40).

3.2. Biological Screening

3.2.1. Materials and Animals

Male Sprague–Dawley rats weighing 250 g and male albino Swiss mice (25 g body weight) were obtained from the animal house of the College of Pharmacy at King Saud University, Riyadh, Saudi Arabia. These animals were kept at room temperature (22±2°C) in a light–controlled room with an alternating 12 h light/dark cycle. Animals were allowed to become acclimatized to laboratory conditions before experimentation and allowed free access to standard food and water. The tested compounds were prepared as suspension in vehicle (0.5% methyl cellulose) and celecoxib was used as a standard drug. The positive control group animals received the reference drug while the negative control received only the vehicle. All procedures were performed with the approval of the Institutional Animal Care and Use Committee. An enzyme immunoassay (EIA) kit (catalog no. 560101, Cayman Chemicals Inc., Ann Arbor, MI, USA) was used in the in vitro cyclooxygenase inhibitory study.

3.2.2. *In vivo* Anti-inflammatory Screening

The anti-inflammatory of the tested compounds were evaluated using in vivo rat carrageenan–induced foot paw

edema model reported previously [23]. Male Sprague–Dawley rats (250 gm body weight) were fasted with free access to water at least 16 h prior to experiments oedema was produced by injecting 0.2 mL of a solution of 1% λ -carrageenan in the hind paw. Paw volume was measured by water displacement with a plethysmometer (UGO BASILE) before, 1, 2 and 3 h after treatment. The tested compounds and reference drug celecoxib were administered intraperitoneally with a 1 mL suspension of test compound in vehicle (0.5% methyl cellulose). The ED₅₀ was measured after 3 hours of treatment with carrageenan, at which maximum percentage of inhibition of carrageenan–induced oedema was reached along with celecoxib. Values reported as mean \pm S.E.M. and significant differences were calculated using ANOVA.

4. Molecular Docking

The rigid molecular docking studies were performed by using HEX 6.1 software, is an interactive molecular graphics program to understand the drug–COX–II interactions. The Structure of the drug was sketched by CHEMSKETCH (<http://www.acdlabs.com>) and converted to pdb format. The crystal structure of the B–DNA dodecamer (CGCGAATTCGCG)2 (PDB ID: 3NT1) was downloaded from the protein data bank (<http://www.rcsb.org/pdb>). All calculations were carried out on an Intelpentium4, 2.4 GHz based machine running MS Windows XP SP2as operating system. Visualization of the docked pose has been done by using CHIMERA (<http://www.cgl.ucsf.edu/chimera/>) molecular graphics program.

5. Conclusion

The synthesized sulfur, halogen and nitrogen derivatives of 1,2,4–triazines have shown promising anti–inflammatory and antimicrobial activities. Out of twelve active compounds, two of them (8 and 10) have shown very anti–inflammatory, anti–microbial activities as well as molecular modeling studies were proved that two analogues showed inconsequential recognition at the binding site of COX–II binding pocket.

References

- [1] Mavrova A. T., Wesselinova D., Tsenov Y. A., Denkova P., *Eru. J. Med. Chem.* 44 (2009) 69.
- [2] Poulomi M., Anita P., Manabendra P.B., Ajaya K. B., *Chem. Rev.*, 114 (2014) 2942.
- [3] Riveiro, M. E., Kimpe, N. D., Moglioni, A.; Vazquez, R. Monczor, F., Shayo, C., Davio, C., *Curr. Med. Chem.* 17 (2010) 1325.
- [4] Kulkarni, M. V., Kulkarni, G. M., Lin, C. H., Sun C. M., *Curr. Med. Chem.* 13 (2006) 2795.
- [5] Katiyar, D., Singh, L. K., *Curr. Med. Chem.* 18 (2011) 2174.
- [6] Sobhi M. G., Fathy M. A., Aly H. A., Peter M., *Heterocycles.* 92 (2016) 945.
- [7] Mamolo M. G., Falagiani V., Zampieri D., Vio L., Banfi, E., *Farmaco*, 55 (2000) 590.
- [8] Schleiss M., Eickhoff J., Auerochs S., Leis M., Abele S., Rechter S., Choi Y., *Antiviral Res.* 79 (2008) 49.
- [9] Russell M. G., Carling R. W., Street L. J., Hallett D. J., Goodacre S., Mezzogori E., Reader M., Cook S. M., Bromidge F. A., Newman R., Smith A. J., Wafford K. A., Marshall G. R., Reynolds D. S., Dias R., Ferris P., Stanley J., Lincoln R., Tye S. J., Sheppard W. F., Sohal B., Pike A., Dominguez M., Atack J. R., Castro J. L., *J. Med. Chem.* 49 (2006) 1235.
- [10] Gregory L. B., Donna M. N., Branko S. J., *Bioorganic & Medicinal Chemistry.* 22 (2014) 4629.
- [11] Dolzhenko A. V., Tan B. J., Chiu G. N., Chiu W. K., *J. Fluorine Chem.* 129 (2008) 242.
- [12] Ali T. E. S., *Eur. J. Med. Chem.* 44 (2009) 4539.
- [13] Abdel–Monem W. R., Abdel–Rahman R. M., *Inter. J. Chem.* 16 (2006) 1.
- [14] El–Gendy Z., Morsy J., Allimony H., Abdel–Monem W. R., Abdel–Rahman R. M., *Sulfur and Silicon.* 178 (2003) 2055.
- [15] Anas M. H. S, Ashok K. S, Nulgumnalli M. R, Rajashri R. N., *Med. Chemistry.* 12 (2016) 90.
- [16] Radwan E., Reem I. A., *Molecules.* 20 (2015) 5374.
- [17] El–Gendy Z., J Morsy, Allimony H., Abdel–Monem W. R., Abdel–Rahman R. M., *Inter. J. Chem.* 178 (2003) 2055.
- [18] Abdel–Rahman R. M., Abdel–Monem W. R., *Indian J. Chem.* 46B (2007) 838.
- [19] Barry A. L., Thomsbery C., Susceptibility testing diffusion testes procedure in Manual of clinical Microbiology, American Society for Microbiology, Washington, (1981) 561.
- [20] El–Haggar R., Al–Wabli R. I., *Molecules.* 20 (2015) 5374.
- [21] Santosh S. C., Chandra shekhar D. U., *Arabian J. Chem.* (2012) In Press.
- [22] Kelsey, C., Duggan, K., Walters, Musee, J., Harp, J., Kiefer, J., Oates, J., Marnett, L. J., *Biol. Chem.* 285 (2010) 34950.
- [23] El–Sayed M. A–A., Abdel–Aziz N. I., Abdel–Aziz A. A–M., El–Azab A. S., Asiri Y. A., El–Tahir K. E. H, *Bioorg. Med. Chem.* 19 (2011) 3416.